

# 01 Polarization interaction of a Rydberg electron with an atomic core in the Thomas–Fermi–Patil model

© A.S. Kornev

Voronezh State University, Voronezh, Russia

e-mail: a-kornev@yandex.ru

Received September 12, 2023

Revised September 25, 2023

Accepted September 28, 2023

Using the Thomas–Fermi–Patil method, a model potential of a Rydberg electron moving in the field of an atomic core with closed shells is obtained. Quantum defects of Rydberg states are calculated in the WKB approximation. The necessity of jointly taking into account the screened and polarization components of the model potential is demonstrated. The values of the „cutoff“ radius in the formula for the polarization potential for a Rydberg electron are found. The limits of applicability of the Thomas–Fermi–Patil method for calculating quantum defects have been clarified: the cores of alkali atoms K, Rb, Cs from group 1 and similar singly charged alkaline earth ions  $\text{Ca}^+$ ,  $\text{Sr}^+$ ,  $\text{Ba}^+$  from group 2 of the Periodic table. Here, significantly penetrating  $s$ ,  $p$  and  $d$  states of a Rydberg electron have the quantum defect exceeding unity. The proposed approach can be used in testing the accuracy of various density functionals and model potentials.

**Keywords:** penetrating Rydberg states, quantum defects, polarization interaction, Thomas–Fermi–Patil model.

DOI: 10.61011/EOS.2023.10.57754.5553-23

## Introduction

The Rydberg atoms (ions) are excited atoms (ions), wherein one or several electrons have a big principal quantum number (up to  $n \sim 1000$ ) [1]. Despite the discovery of the Rydberg series in the atomic spectra by I.J. Balmer in 1885, the interest to the Rydberg states has only grown for the last two decades [2]. These atoms have specific properties, in particular, abnormally high response to impact of external electromagnetic fields and a long lifetime.

The Rydberg atoms (RAs) are important for the fundamental physics. For example, the radiation lifetimes of the atoms in the meta-stable Rydberg states in the optical traps [3] are required both to understand the data obtained from the astrophysical observations of the interstellar space and to test the Standard Model [4]. The diamagnetic susceptibilities in RAs reach abnormally high values  $\sim n^4$  [5]. The large sizes ( $\sim 1 \mu\text{m}$ ) and the high susceptibilities of RAs determine the most important properties of plasma [6]. It results in manifestation of new non-linear properties of the Rydberg matter, for example, dipole blockade [7], electro-induced transparency [8] and substantially non-linear behavior of the interacting RAs at the level of individual optical photons [9–13]. The various RA application areas include high-precision measurements [14,15].

The RA spectrum is similar to the hydrogen one with replacement  $n \rightarrow n - \mu$ , where  $\mu$  is the quantum defect (QD) being the main characteristic of the Rydberg states. Therefore, the RAs are suitable for theoretical study. However, it is difficult to obtain a radial wave function

of the Rydberg electron (RE) due to a large number of its oscillations ( $\sim n$ ). Thus, there is a problem of obtaining the QD values and understanding the mechanisms of its occurrence. The first accurate calculations of the Rydberg spectrum of magnesium were performed in the paper [16] with the close-coupling method taking into account Coulomb, multipole and polarization interactions. The similar results for neon were obtained in the paper [17] using the Kohn–Sham functional. The Rydberg spectrum of calcium was calculated in the paper [18] with the self-consistent field method. The paper [19] has studied the atoms of the carbon group using the  $R$ -matrix approach. At last, the recent calculations of the Rydberg spectra have widely used various model potentials [20]. The substantial drawback of the listed methods is their application to a specific atom only.

It would have been convenient to obtain the model potential of the RE numerically with the Thomas–Fermi (TF) method. This statistical method can be considered as a semi-classical limit of the Hartree–Fock equations. In the recent decades, the TF method has been successfully used in investigating the properties of heated plasma under the external electromagnetic fields [21,22]. However, the TF method poorly reproduces the electron density near the nucleus and at the periphery of the core of the residual ion. These are the domains which are important for the calculations of the RE spectra. There were numerous attempts to improve the TF method [23–26]. It seems that the most suitable implementation of the TF model for practical application is its modification proposed by S. Patil [27,28]. Hereinafter, this implementation of the

TF method will be referred to as the Thomas–Fermi–Patil (TFP) model.

The polarization potential of the core noticeably affects the RE motion [29]. Usually, its analytical formula contains free parameters. The correlation polarization potential without the free parameters has been obtained for scattering of electrons on the atoms in [30]. But, the authors of [30] were limited themselves to the helium atom.

The first successful QD calculations within the framework of the TFP model have been performed by the author for some atoms and ions in the paper [31]. However, the recently-obtained new data on the Rydberg levels in [32] make it possible to study in more detail QDs and polarization interaction of RE with the core, thereby substantially enlarging the set of the studied atoms and ions.

This study is aimed at developing a simple single-particle method of the model potential for calculating QDs of the Rydberg states of a single electron moving above the core consisting of closed shells. Such systems are exemplified by the atoms of groups 1, 11 and ions of the elements of groups 2, 12 of the Periodic table. These atoms and ions are often used in the physics of the Rydberg states [12,33]. The TFP method will underlie the research. After comparison of the results with reference data, the calculations and analysis of the parameters of the polarization interaction of RE with the core will be performed. It will result, in addition to [31], in refinement of limits of applicability of the TFP method.

The required formulas are derived in Section 1. Subsection 1.1 describes a general structure of the RE model potential and lists the properties of the polarization component. Subsection 1.2 specifies the TFP method for calculating the screened and polarization components of the RE potential. Subsection 1.3 derives the WKB formula of the RE quantum defect in the model potential. The numerical results are given and discussed in Section 2. The quantum defects are analyzed in Subsection 2.1, the «cutoff» radii of the polarization potential are considered in Subsection 2.2. The main conclusions are given in Conclusion. The cumbersome intermediate calculations used in derivation of the quantum defect formula are given in Appendix. Hereinafter, unless specified otherwise, the atomic system of units is used ( $\hbar = e = m_e = 1$ ).

## 1. Theoretical model for calculation of quantum defects

The present paper deals with the RE motion in a neutral atom of the alkali element, in a single-charged cation of the alkaline earth element, etc. In this case, the RE is affected by the Coulomb field of the point nucleus with the charge number  $Z$  and the electrostatic field of the  $N_c$ -electron core of the residual ion consisting on the closed shells only. Therefore, there is no nonlocal exchange interaction in the RE Hamiltonian, thereby making it possible to restrict ourselves to a potential approach when describing the RE motion. It means that the electron will move in a certain

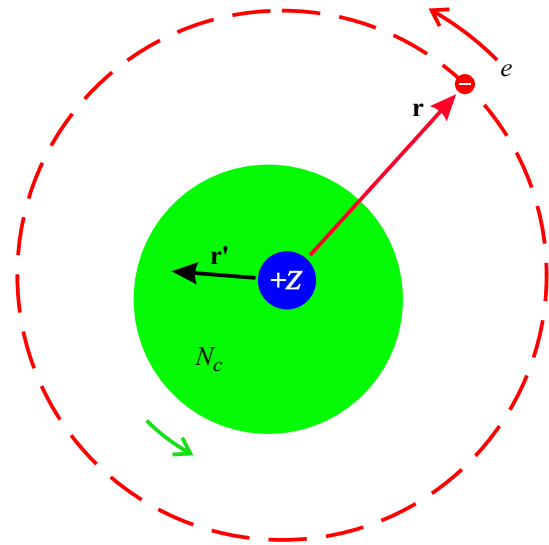


**Figure 1.** Polarization of the core by the Rydberg electron.

central field  $V_{\text{Ryd}}(r)$ , which has no multipole component and satisfies the condition

$$V_{\text{Ryd}}(r) \rightarrow \begin{cases} -Z/r, & \text{for } r \rightarrow 0, \\ -z/r, & \text{for } r \rightarrow \infty. \end{cases} \quad (1)$$

Here,  $z = Z - N_c$  is the charge of the residual ion. For the neutral atom  $z = 1$ , for the single-charged ion  $z = 2$ , etc.

### 1.1. Model potential of the Rydberg electron

This subsection analyzes the structure of the model potential  $V_{\text{Ryd}}(r)$ . It can be assumed that the RE potential in the atom (or the ion) consists of the two terms:

$$V_{\text{Ryd}}(r) = -\phi_{\text{scr}}(r) - \phi_{\text{polar}}(r). \quad (2)$$

Here  $\phi_{\text{scr}}(r)$  is the potential of the residual ion. It is the potential of the nucleus incompletely screened by the core shells, so it obeys the boundary conditions:

$$r\phi_{\text{scr}}(r) \approx \begin{cases} Z, & \text{for } r \rightarrow 0, \\ z + h(r)e^{-qr}, & \text{for } r \rightarrow \infty, \end{cases} \quad (3)$$

where  $q > 0$  is a certain constant of screening, the function  $h(r)$  can increase not faster than the exponential. The potential  $\phi_{\text{scr}}(r)$  has no multipole component due to spherical symmetry of the core.

The term  $\phi_{\text{polar}}(r)$  is caused by reverse impact of the RE on the core of the remaining ion. There is electrostatic repulsion between the RE and the core, so the core is somewhat deformed (Fig. 1). In other words, the RE Coulomb field causes deformation (or polarization) of the core. The core deformation results in an additional term  $\phi_{\text{polar}}(r)$  in the potential, which additionally affects the RE.

To obtain an explicit form of  $\phi_{\text{polar}}(r)$ , first of all, it is necessary to investigate the core response to the external

electrostatic field with the potential  $V(\mathbf{r})$ . Its the  $2^L$ -pole component  $V_L$  has the following form:

$$V_L(\mathbf{r}) = -\xi_L \sum_{i=1}^{N_c} r_i^L P_L(\cos \theta_i), \quad (4)$$

where the angle  $\theta_i$  specifies orientation of the radius-vector of the  $i$ -electron  $\mathbf{r}_i$  with respect to the electric vector of the dipole component,  $P_L$  is the Legendre polynomial,  $\xi_L$  is a small parameter.

If the field strength (4) is much less than the inter-atom one, then the core potential gets a little addition

$$\delta\phi_L(\mathbf{r}) = \xi_L \eta_L(r) P_L(\cos \theta) = \xi_L \sqrt{\frac{4\pi}{2L+1}} \eta_L(r) Y_{L0}(\hat{\mathbf{r}}), \quad (5)$$

where  $\hat{\mathbf{r}} \equiv \mathbf{r}/r$ ,  $Y_{LM}(\hat{\mathbf{r}})$  is the spherical harmonic, and the function  $\eta_L(r)$  meets the boundary conditions:

$$\eta_L(r) \approx \begin{cases} a_L r^L, & \text{for } r \rightarrow 0, \\ r^L - \alpha_L / r^{L+1}, & \text{for } r \rightarrow \infty, \end{cases} \quad (6)$$

where  $a_L$  and  $\alpha_L$  are the constants to be defined.

The electron density  $\rho(\mathbf{r}) > 0$  is related to the electrostatic potential  $\phi(\mathbf{r})$  in any point of space via the Poisson equation:

$$\nabla^2 \phi(\mathbf{r}) = 4\pi \rho(\mathbf{r}).$$

Outside the charge distribution region, the Poisson equation becomes homogeneous and transforms to the Laplace equation. The solid harmonics  $r^L Y_{LM}(\hat{\mathbf{r}})$  and  $r^{-L-1} Y_{LM}(\hat{\mathbf{r}})$  satisfy the Laplace equation, so, in accordance with (5), (6)

$$\nabla^2 \delta\phi_L(\mathbf{r}) \approx 0, \quad r \rightarrow 0, \infty.$$

The next step will include calculation of a correction to energy of Coulomb interaction of RE with the core, which is caused by polarization. It should be done by using multipole expansion of the Coulomb potential created by RE:

$$|\mathbf{r} - \mathbf{r}'|^{-1} = \sum_{L=0}^{\infty} \frac{r_{<}^L}{r_{>}^{L+1}} P_L(\cos \theta), \quad (7)$$

where  $\mathbf{r}$  is the RE coordinate,  $\mathbf{r}'$  is the coordinate of the observation point of the RE electric field (Fig. 1),  $r_{<} = \min(r, r')$ ,  $r_{>} = \max(r, r')$ ,  $\theta = \widehat{(\mathbf{r}, \mathbf{r}')}.$

The classical speed of the RE in the Bohr orbit is much less than the electron speeds inside the core, so, it can be concluded that core configuration does «follow» the Rydberg electron. This situation is partially similar to the applicability condition of the Born–Oppenheimer approximation in the molecule. Thus, the retardation effects for the atom's electromagnetic field can be neglected to restrict ourselves to taking into account only the electrostatic effects. Since the radius of the classical Rydberg orbit substantially exceeds the core radius, then in the expansion (7) it is enough to assume that  $r_{<} = r'$ ,  $r_{>} = r$ . After this, the expansion (7) will be similar to (4) with the small parameter

$\xi_L = -r^{-L-1}$ . The smallness of polarization interaction makes it possible to independently consider the contribution of each multipole component.

The correction  $\delta\phi_L$  comprises not only the change of the potential created by the core deformation, but a disturbing potential created by the RE (see the boundary condition (6) at  $r \rightarrow \infty$ ). Therefore,  $\phi_{\text{polar}}$  will be obtained by excluding this self-action from  $\eta_L$ . As a result,

$$\phi_{\text{polar}}(r) \approx \frac{1}{2} \sum_{L=1}^{\infty} \frac{r^L - \eta_L(r)}{r^{L+1}}. \quad (8)$$

There is no analytical formula for  $\eta_L(r)$ . Nevertheless, in accordance with (6), the asymptotic correction to the RE potential caused by the dipole component is provided by a comparatively simple model formula

$$\phi_{\text{polar}}(r) \approx \frac{\alpha_1}{2r^4}, \quad r \rightarrow \infty \quad (9)$$

where  $\alpha_1$  is the dipole polarizability of the core [34]. The formula (9) neglects the contribution of the highest multipoles, i.e. only a long-range component is taken into account. It should be noted that in the case of the open-shell core with a non-zero total orbital momentum the polarization potential at infinity would decrease more slowly:  $\phi_{\text{polar}}(r) \sim r^{-3}$ .

It is impossible to directly use the model formula (9) instead of (8) in calculation of the RE spectrum due to electron drop to the center in the field  $\sim r^{-4}$  when  $r \rightarrow 0$ . Therefore, in practice the expression (9) is «cut off» in the vicinity zero, i.e. it is replaced by a zero-regular expression

$$\phi_{\text{polar}}(r) \approx \frac{\alpha_1}{2r^4} \left(1 - e^{-r^6/r_c^6}\right), \quad (10)$$

containing the free parameter  $r_c$ . This parameter (the «cutoff» radius) is selected empirically, for example, to obtain the result stable to its variations and having a core size's order. The expression (10) is often used to describe interaction of the atom with slow charged particles. In addition to (10), there are other forms of regularization of  $\phi_{\text{polar}}(r)$ , for example:

$$\phi_{\text{polar}}(r) \approx \frac{\alpha_1 r^2}{2(r_c^2 + r^2)^3}, \quad (11)$$

$$\phi_{\text{polar}}(r) \approx \frac{\alpha_1}{2(r_c^2 + r^2)^2}. \quad (12)$$

It should be noted that the «exact» expression (8) also requires regularization in zero, since it has been obtained in the approximation  $r \gg r'$ . The perturbation approach cannot be applied outside this approximation. The regularization (8) is detailed in the next subsection.

Thus, for practical calculations of the RE spectra, the potential approach will include the use of the screened potential of the nucleus  $\phi_{\text{scr}}(r)$  and the dipole polarizability of the core  $\alpha_1$ .

**1.2. Thomas–Fermi–Patil method**

The present subsection specifies the modern modification of the statistical TF method for calculating the screened  $\phi_{scr}$  and polarization  $\phi_{polar}$  components of the potential (2).

**1.2.1. Screened potential** The TF method is one of the those for obtaining the potential  $\phi_{scr}$ , which is created by the nucleus with the charge  $Z$  and by the core with the  $N_c$  electrons in the Rydberg atom or ion. This method requires solving the single differential equation instead of the system of Hartree-Fock equations.

As known, the TF method is based on the Poisson equation, which for the spherically symmetrical distribution of the screening charge has the following form

$$\frac{1}{r} \frac{d^2}{dr^2} [\phi_{scr}(r)] = 4\pi\rho_0(r), \tag{13}$$

where  $\rho_0(r)$  is the local electron density in the core. The Teletrons in the TF model are presented as a completely degenerate ideal gas that obeys the Fermi–Dirac statistics and stays in the field of the atomic nucleus. Then, the density  $\rho_0$  and the potential  $\phi_{scr}$  will be interrelated by the relationship:

$$\rho_0(r) = \frac{1}{3\pi^2} \{2[\phi_{scr}(r) - E_c]\}^{3/2} + \frac{11}{9\pi^3} \{2[\phi_{scr}(r) - E_c]\}, \tag{14}$$

where  $E_c$  is the core ionization energy. The first term of (14) is of a statistical nature. It was obtained by Thomas [35] and Fermi [36]. The second term takes into account the exchange (Dirac) [37] and quantum (Schwinger) [38] corrections. Therefore, the electron density in the form (14) is sometimes called the Thomas–Fermi–Dirac–Schwinger model (TFDS). It should be noted that the formula (14) is a particular case of the density functional.

The TFDS model (14) is applicable in a classically accessible region, i.e. in case of meeting the condition

$$E_c < \phi_{scr}(r). \tag{15}$$

In other words, the TFDS model can be used within the interval

$$Z^{-1} \lesssim r \lesssim (Z - N_c + 1)^{-1}, \tag{16}$$

wherein the semi-classical approximation can be applied for the core electrons.

However, near the nucleus and at great distances, i.e. when (16) is violated, the formula (14) provides an incorrect result. The point is that together with inapplicability of the semi-classical approximation, these domains also have a low electron density, therefore, the laws of statistical physics are not applicable. The modification of the TFDS method bypassing the said drawback has been proposed by S. Patil

in the papers [27,28]:

$$\begin{aligned} \rho_0(r) = & \left\{ \frac{1}{3\pi^2} \left[ \frac{2r(\phi_{scr} - E_c)}{r + c_1} \right]^{3/2} \right. \\ & \left. + \frac{11}{9\pi^3} \left[ \frac{2r(\phi_{scr} - E_c)}{r + c_1} \right] \right\} \theta(\phi_{scr} - E_c) \\ & + \frac{A}{4\pi} \left( \frac{2\kappa r}{2\kappa r + 1} \right)^v \left( r + \frac{1}{2\kappa} \right)^{-2\beta} \\ & \times \left( 1 - \frac{\kappa c_2}{2\kappa r + 1} \right)^2 \% e^{-2\kappa r}. \end{aligned} \tag{17}$$

Here,

$$\kappa = \sqrt{2E_c}, \quad \beta = 1 - z/\kappa, \quad z = Z - N_c + 1$$

is the charge of the residual ion. The Heaviside function  $\theta(\phi_{scr} - E_c)$  provides for meeting the condition (15), and, therefore, the first term of (17) describes the local electron density in the classically accessible region of the electron motion. The constant  $c_1$  is introduced to describe the charge density near the nucleus. Its value can be obtained by numerical solving the equation

$$\begin{aligned} & \left[ 3 \left( \frac{2Z}{c_1} \right)^{1/2} + \frac{22}{3\pi} \right] \left[ g'(0) - E_c - \frac{Z}{c_1} \right] \\ & = -(2Z)^2 \% \left[ \left( \frac{2Z}{c_1} \right)^{1/2} + \frac{11}{3\pi} \right], \end{aligned} \tag{18}$$

$$g(r) = r\phi_{scr}(r)$$

by the iteration method with selecting  $c_1 \simeq 0.95Z^{-1.05}$  as a zero approximation. Namely, first of all, the equation (13) is solved with the right-hand side as (17) and with the value  $c_1$  as the zero approximation; then, the first approximation for  $c_1$  is derived from the equation (18). Next, the cycle is repeated until the difference between subsequent values of  $c_1$  becomes smaller than a specified value. The difference between the exact and initial values of  $c_1$  can be up to 10%. Thus, the TFP method comprises elements of the self-consistent field method. The factor  $r/(r + c_1)$  is introduced to eliminate singularity at zero.

The second term of (17) describes the asymptotic form of the electron density away from the nucleus in the classically forbidden region of motion. For the large and small values of  $N_c$

$$v = \begin{cases} 2, & \text{for } 2 \leq N_c \leq 17, \\ 4, & \text{for } N_c \geq 18. \end{cases}$$

The constant  $c_2$  is determined by the orbital quantum number of the electron in the outermost shell of the core  $l_c$  by the formula

$$c_2 = \frac{1}{\kappa} (\beta + l_c)(\beta - l_c - 1) - \frac{1}{2\kappa} (v + 2\beta). \tag{19}$$

The value of the constant  $A$  can be found from the first boundary condition (3) to the equation (13):

$$r\phi_{\text{scr}}(r) \rightarrow Z, \quad r \rightarrow 0. \quad (20)$$

In practical calculations, zero can be replaced by a small distance to the nucleus, for example,  $\sim 10^{-6}$  Bohr.

The second boundary conditions follows from (3). It is caused by behavior of the electron density at infinity and within the framework of the TFP model [28] it takes the form:

$$r\phi_{\text{scr}}(r) \rightarrow Z - N_c + A \left[ f(v + 2\beta) - c_2 f(v + 2\beta + 1) + \frac{1}{4} c_2^2 f(v + 2\beta + 2) \right], \quad (21)$$

$$r \rightarrow \infty,$$

where

$$f(a) \rightarrow \left\{ \frac{1}{(2\kappa)^2} + \frac{2}{(2\kappa)^3} \left[ \frac{v+1}{r} - \frac{2\kappa a}{2\kappa r + 1} \right] + \frac{3}{(2\kappa)^4} \left[ \frac{v+1}{r} + \frac{4\kappa^2 a(a+1)}{(2\kappa r + 1)^2} - \frac{4\kappa a(v+1)}{r(2\kappa r + 1)} \right] + \dots \right\} \times \frac{r^{v+1}}{(r + 1/2\kappa)^a} e^{-2\kappa r}.$$

In practice, the present study replaces infinity with the distance  $\sim 4N_c^{1/3}$  Bohr, which substantially exceeds the core radius.

Taking into account (17), the Poisson equation (13) becomes non-linear.

Thus, the modification proposed by Patil introduces two additional parameters into the traditional TFDS model containing only the parameters  $Z$  and  $N_c$ , as follows:  $l_c$  and  $E_c$ . Unlike the TFDS model, the TFP model formally cancels the limitations (15) and (16). In particular, the TFP model correctly reproduces the electron density at the core periphery and can be used for solving the problems, which require the wave functions in the asymptotically remote region, for example, when investigating interaction of the atoms with optical radiation. However, actual applicability of the TFP requires additional investigation.

**1.2.2. Polarization corrections** If the residual ion is subjected to impact of the  $2^L$ -pole potential (4), then its electron configuration is deformed resulting in polarization. If the potential (4) is small as compared to the field inside the core, then its influence can be regarded as perturbation and taken into account by a respective correction to the local electron density in the TFP model:

$$\phi \rightarrow \phi_{\text{scr}} + \delta\phi_L = \phi_{\text{scr}} + \eta_L(r)P_L(\cos\theta).$$

The function  $\eta_L(r)$  can be obtained by solving the non-linear equation [28]:

$$\frac{1}{r} \frac{d^2}{dr^2} (r\eta_L) - \frac{L(L+1)}{r^2} \eta_L = 4\pi \left\{ \frac{1}{2\pi^2} \left[ \frac{2r}{r+c_1} \right]^{3/2} \times (\phi_{\text{scr}} - E_c)^{1/2} + \frac{11}{9\pi^3} \left[ \frac{2r}{r+c_1} \right] \right\} \theta(\phi_{\text{scr}} - E_c) \eta_L + \frac{2Ar^{L+1}}{\kappa(L+1)} \left( \frac{2\kappa r}{2\kappa r + 1} \right)^v (r + 1/2\kappa)^{-2\beta} \times \left[ 1 - \frac{\kappa c_3}{2\kappa r + 1} \right]^2 e^{-2\kappa r}. \quad (22)$$

Here, the constant  $c_3$  is defined similarly to  $c_2$  (19):

$$c_3 = -(v + 2\beta)/2\kappa.$$

Only the solutions (22) meeting the boundary conditions (6) are selected. The constants  $a_L$  and  $\alpha_L$  are obtained from the equations

$$\eta_L(R_0) = R_0^L - \frac{\alpha_L}{R_0^{L+1}}, \quad \eta'_L(R_0) = LR_0^{L-1} + (L+1) \frac{\alpha_L}{R_0^{L+2}}, \quad (23)$$

whence

$$\alpha_L = \frac{R_0^{L+1}}{L+1} [R_0 \eta'_L(R_0) - LR_0^L]. \quad (24)$$

The constant  $a_L$  is implicitly included in (23) via  $\eta_L$ . The distance  $R_0$  is selected larger as compared to the core radius (as mentioned above, the present paper specifies it to be  $R_0 \approx 4N_c^{1/3}$ ). The constant  $\alpha_L$  is mentioned in [28] as the  $2^L$ -pole polarizability (at  $L=1$  it coincides with the usual dipole polarizability  $\alpha$ ; at  $L=2$  it differs from the usual hyperpolarizability  $\gamma$  by the constant factor:  $\alpha_2 = \gamma/48$ ).

The polarization interaction (8) in the TFP model is regularized in the same way as the density (17):

$$\phi_{\text{polar}}(r) \approx \frac{1}{2} \left( \frac{r}{r+c_1} \right)^v \sum_{L=1}^{\infty} \frac{r^L - \eta_L(r)}{r^{L+1}}. \quad (25)$$

As shown by the calculations, the polarization corrections are mainly contributed only by the dipole component  $\phi_{\text{polar}}$ , i.e. it is enough to take into account only  $V_L(r)$  with  $L=1$ . The contribution of the non-dipole terms  $V_L(r)$  into  $\phi_{\text{polar}}$  usually does not exceed  $\sim 0.1\%$ .

### 1.3. WKB formula of the quantum defect

It is convenient to describe the RE energy spectrum due to the Coulomb asymptotic form of the potential  $V_{\text{Ryd}}(r)$  at  $r \rightarrow \infty$  with the following formula

$$E_{nl} = -\frac{z^2}{2v_{nl}^2}, \quad (26)$$

where  $n$  and  $l$  are the principal and orbital quantum numbers, respectively,

$$v_{nl} = n - \mu_{nl}$$

is the effective principal quantum number (non-integer),  $\mu_{nl}$  is the quantum defect, which in case of meeting the conditions

$$n \gg \max(l, 1) \tag{27}$$

ceases to depend on  $n$ :

$$\lim_{n \rightarrow \infty} \mu_{nl} = \mu_l. \tag{28}$$

Calculation of the QD  $\mu_l$  is the primary aim of this subsection.

Without taking into account the spin, the RE wave function in the states with the given values of the squared orbital momentum and its projection is factorized into a radial and angular parts:

$$\psi_{nlm_l}(\mathbf{r}) = \frac{1}{r} R_{nl}(r) Y_{lm_l}(\hat{\mathbf{r}}),$$

where  $m_l$  is the magnetic quantum number.

The radial wave function  $R_{nl}(r)$  satisfies the radial Schrödinger equation taking into account (26)

$$-\frac{1}{2} \frac{d^2 R_{nl}}{dr^2} + \left[ \frac{l(l+1)}{2r^2} + V_{\text{Ryd}}(r) \right] R_{nl} = -\frac{z^2}{2v_{nl}^2} R_{nl} \tag{29}$$

and is normalized to the unity by the condition

$$\int_0^\infty R_{nl}^2(r) dr = 1.$$

The excited states of the alkali atoms were investigated in the model potential in the pioneering study [39]. The potential  $V_{\text{Ryd}}(r)$  was obtained there within the Thomas–Fermi method accounting for the Amaldi correction [40]. In order to rectify the influence of the incorrect form of  $V_{\text{Ryd}}(r)$  at the core periphery, the authors of [39] used specific schemes for solving the radial Schrödinger equation (29). The present paper will use the potential  $V_{\text{Ryd}}(r)$  found with the TFP method. The equation (29) will be solved in the WKB approximation. This approach is more simple as compared to [39].

As well-known, for the highly-excited states in the potential with the Coulomb asymptotic form, the WKB approximation is always applicable. The Rydberg states satisfy this condition (see (1) and (27), as well as [41]). However, for the central field, the WKB formulas somewhat differ from the case of one-dimension motion. In particular, the Bohr–Sommerfeld formula takes the form [42]:

$$\int_{r_1}^{r_2} p_{nl}(r) dr = \pi(n - \mathcal{L}_l), \quad n = l + 1, l + 2, \dots \tag{30}$$

Here, the classical momentum is given by the expression

$$p_{nl}(r) = \sqrt{2} \left[ -\frac{z^2}{2v_{nl}^2} - V_{\text{Ryd}}(r) - \frac{\mathcal{L}_l^2}{2r^2} \right]^{1/2},$$

$r_{1,2}$  are the classical turning points, wherein  $p_{nl}$  goes to zero (in the  $s$ -states it is assumed that  $r_1 = 0$ ),

$$\mathcal{L}_l = (1 - \delta_{l0}) \left( l + \frac{1}{2} \right). \tag{31}$$

In the states with  $l > 0$  the value  $\mathcal{L}_l$  differs from the exact value  $\sqrt{l(l+1)}$ , thereby resulting in an additional term  $1/(8r^2)$  appearing in the centrifugal potential. However, when  $\mathcal{L}_l$  is selected as specified in (31), it provides exact values both for the energies of the bound states and for the scattering phases when the electron moves in a purely Coulomb field of attraction.

The equation (30) is scarcely suitable for numerical calculation of QDs. With the growth of  $n$ , the classical turning point is shifted to infinity as  $r_2 \sim n^2/z$ , while the integrand  $p_{nl}(r)$  is still a limited magnitude, due to an asymptotic form of (1). Thus, the value of the integral is unlimited and it monotonically increases with increase of  $n$ . The right-hand side of the equation (30) linearly depends on  $n$ . Therefore, for the case of infinitely large values of  $n$ , computer numerical solving the equation (30) can exhibit both accuracy loss and bit overflow.

This problem can be solved quite simply, if the potential  $V_{\text{Ryd}}(r)$  is represented in accordance with (1) as

$$V_{\text{Ryd}}(r) = v_{\text{Ryd}}(r) - \frac{z}{r},$$

where  $v_{\text{Ryd}}(r)$  is the short-range component, which decreases faster than  $\sim r^{-2}$  at large distances.

Let  $r_1 < R < r_2$  be a finite radius of action of the component  $v_{\text{Ryd}}(r)$ , starting from which it can be neglected to transform the integral in the equation (30) into the following form:

$$\int_{r_1}^{r_2} p_{nl}(r) dr = \int_{r_1}^R p_{nl}(r) dr + \int_R^{r_2} p_{nl}^{(0)}(r) dr, \tag{32}$$

where  $p_{nl}^{(0)}(r)$  is the classical electron momentum in the pure Coulomb potential, which differs from  $p_{nl}(r)$  by replacement

$$V_{\text{Ryd}}(r) \rightarrow -z/r.$$

The second integral of (32) can be analytically evaluated by the replacement

$$r = r(\varphi) = a_{nl}(1 - \epsilon_{nl} \cos \varphi), \tag{33}$$

where

$$a_{nl} = \frac{v_{nl}^2}{z}, \quad \epsilon_{nl} = \sqrt{1 - \frac{M_l^2}{v_{nl}^2}}$$

are the parameter and eccentricity of the electron classical orbit, respectively. Such replacement is used in [43] when solving the classical Kepler’s problem. After (33) done, the integration limits are transformed into the form:

$$R \rightarrow \varphi_{nl} = \arccos \left[ \frac{1}{\epsilon_{nl}} \left( 1 - \frac{R}{a_{nl}} \right) \right], \quad r_2 \rightarrow \pi.$$

The final analytical expression for the second integral in (32) has a quite cumbersome but elementary form (see Appendix):

$$\int_R^{r_2} p_{nl}^{(0)}(r) dr = \pi(v_{nl} - M_l) - v_{nl}(\varphi_{nl} + \epsilon_{nl} \sin \varphi_{nl}) + 2\mathcal{L}_l \arctan \left[ \frac{\mathcal{L}_l}{v_{nl}(1 - \epsilon_{nl})} \tan \frac{\varphi_{nl}}{2} \right]. \quad (34)$$

Under the condition (27), the formula (34) can be simplified by expanding the right-hand side into the Taylor series in powers of the small parameters  $\mathcal{L}_l/v_{nl}$  and  $zR/v_{nl}^2$  and neglecting the terms  $O(v_{nl}^{-1})$  (see Appendix):

$$\int_R^{r_2} p_{nl}^{(0)}(r) dr \approx \pi(n - \mu_{nl} - \mathcal{L}_l) - 2\mathcal{L}_l(\Xi_l - \arctan \Xi_l), \quad (35)$$

where

$$\Xi_l = \sqrt{\frac{2zR}{\mathcal{L}_l^2} - 1}. \quad (36)$$

It is clear from (35) that as  $n$  increases, the integral will infinitely increase only due to the term  $\pi n$ . The other terms except for  $\mu_{nl}$  will not depend on  $n$  at all.

After substitution of (35) into (32), the terms  $\pi n$  of the Bohr–Sommerfeld equation (30) cancel each other out. In the limit  $n \rightarrow \infty$ , the Bohr–Sommerfeld equation provides an explicit formula for the QD, which ceases to depend on  $n$  in accordance with (28):

$$\pi\mu_l = \int_{r_1}^R p_l(r) dr - 2\mathcal{L}_l(\Xi_l - \arctan \Xi_l). \quad (37)$$

Here,

$$p_l(r) = \lim_{n \rightarrow \infty} p_{nl}(r) = \sqrt{2} \left[ -V_{\text{Ryd}}(r) - \frac{\mathcal{L}_l^2}{2r^2} \right]^{1/2},$$

and the quantity  $\Xi_l$  is defined by (36).

In case of the  $s$ -states ( $l = 0$ ), the expression (37) will be formally transformed by the limit transition  $\mathcal{L}_l \rightarrow 0$ :

$$\pi\mu_s = \int_{r_1}^R p_s(r) dr - \sqrt{8zR}, \quad (38)$$

where

$$p_s(r) = \sqrt{-2V_{\text{Ryd}}(r)}.$$

The formulas (37) solve the assigned problem of QD calculation in the WKB approximation. They require numerical integration of the classical momentum over the range of action of the ionic core. In other words, the QD is expressed in quadratures. The radius  $R$  is selected so as to negligibly change the result with its insignificant variation.

It is easy to make sure that if the pure Coulomb potential  $-z/r$  is selected as  $V_{\text{Ryd}}(r)$ , then QD will tend to zero. Thus, the QD is caused the core presence in the potential  $V_{\text{Ryd}}(r)$  and by penetration of RE into this core.

## 2. Numerical results and discussion

This section provides the results of numerical calculation of the QDs and the parameter  $r_c$  in the potential of polarization interaction of RE with the core (10) in several atoms and ions with one highly excited electron above the core with the closed shells. The components of the potential  $V_{\text{Ryd}}(r)$  have been obtained by numerical integration of the differential equations (13) with the boundary conditions (20), (21) and the equations (22) with the boundary conditions (6) in the *Wolfram Mathematica* package with automatic selection of the method and the step. The atoms and ions with the outermost  $s^2$  shell of the core (Li, Be<sup>+</sup>),  $p^6$  shell (Na, Mg<sup>2</sup>, K, Ca<sup>+</sup>, Rb, Sr<sup>+</sup>, Cs, Ba<sup>+</sup>) and  $d^{10}$  shell (Cu, Zn<sup>+</sup>, Ag, Hg<sup>+</sup>) were considered. Only the  $nl_{l+1/2}$ -configurations of the Rydberg electron have been studied.

First of all, the TFP method has been tested by calculating the QDs of the Rydberg states using the formulas (37) and (38). The obtained values were compared with the reference data. Then, the same method was used to find the values of the «cutoff» radius  $r_c$  in the polarization potential (10). The numerical results are given in Tables 1 and 2. The core ionization energy  $E_c$  was taken from [32].

### 2.1. Quantum defects

The quantum defects calculated within the TFP method have been compared with those obtained from the NIST-tabulated reference energy levels  $E_{nl}^{(\text{ref})}$  (in cm<sup>-1</sup>) of the excited states of the atoms and ions [32] at the fixed  $l$  by the formula

$$\mu_{nl}^{(\text{ref})} = n - z \sqrt{\frac{\text{Ry}_M}{E_{nl}^{(\text{ref})} - \text{IL}}}, \quad (39)$$

where IL is the ionization limit,  $\text{Ry}_M = \text{Ry}_\infty / (1 + m_e/M)$ ,  $\text{Ry}_\infty = 109\,737.04$  cm<sup>-1</sup> is the Rydberg constant,  $m_e$  is the electron mass,  $M$  is the nucleus mass. The consideration included the most common stable isotopes.

It should be noted that the information system [44] that is different from the NIST database, has the Rydberg atom levels with the higher values of the principal quantum number  $n$  with the same accuracy as in [32]. However, with the growth of  $n$ , the formula (39) subtracts more and more closer numbers. As a result, the accuracy of QD calculation starts quickly decreasing, if  $n$  exceeds the values from [32]. In this situation, it is impractical to use the information system [44].

The Ritz formula was applied to the quantum defects (39) (it is the asymptotic series):

$$\mu_{nl}^{(\text{ref})} = \mu_l^{(0)} + \mu_l^{(2)}[n - \mu_l^{(0)}]^{-2} + \mu_l^{(4)}[n - \mu_l^{(0)}]^{-4} + \dots \quad (40)$$

The parameters  $\mu_l^{(0)}$ ,  $\mu_l^{(2)}$ ,  $\mu_l^{(4)}$ , ... were obtained by non-linearly fitting the formula (40) to the values of  $\mu_{nl}^{(\text{ref})}$  for the entire set of the involved principal quantum numbers  $n$  by the least-square method. In accordance with the results

**Table 1.** Quantum defects in the atoms and cations  $\mu_l$  and the «cutoff» radii of the polarization potentials of their cores  $r_c$  in the TFP model (see explanations in the text)

Atom (ion)	$E_c$ , eV	$\alpha_1$ , Bohr <sup>3</sup>	Configu- ration	Quantum defect $\mu_l$			$r_c$ , Bohr	$R_i$ , Bohr
				Only $\phi_{scr}$	$\phi_{scr}$ + $\phi_{polar}$	$\mu_l^{(ref)}$		
Li	75.64	0.1923	[He] <i>ns</i>	0.355	0.363	0.400	0.576(3)	1.44
			[He] <i>np</i>	0.007	0.014	0.048	–	
Be <sup>+</sup>	153.9	0.05226	[He] <i>ns</i>	0.233	0.236	0.260	0.374(2)	0.85
			[He] <i>np</i>	0.017	0.022	0.050	–	
Na	47.29	1.001	[Ne] <i>ns</i>	1.266	1.329	1.348	0.826(2)	1.93
			[Ne] <i>np</i>	0.597	0.704	0.855	0.584	
Mg <sup>+</sup>	80.14	0.4533	[Ne] <i>nd</i>	0.000	0.010	0.015	–	1.36
			[Ne] <i>ns</i>	0.996	1.034	1.067	0.567(2)	
K	31.63	5.480	[Ne] <i>np</i>	0.536	0.593	0.695	0.461(1)	2.61
			[Ne] <i>nd</i>	0.004	0.017	0.046	–	
Ca <sup>+</sup>	50.91	3.26	[Ar] <i>ns</i>	2.011	2.123	2.180	1.197(3)	1.89
			[Ar] <i>np</i>	1.431	1.578	1.711	1.140(1)	
Cu	20.29	6.57	[Ar] <i>nd</i>	0.002	0.039	0.277	1.125(1)	1.46
			[Ar] <i>nf</i>	0.000	0.006	0.010	–	
Zn <sup>+</sup>	39.72	3.032	[Ar] <i>ns</i>	1.669	1.747	1.803	0.968(1)	1.40
			[Ar] <i>np</i>	1.243	1.338	1.429(1)	0.898(3)	
Rb	27.29	9.211	[Ar] <i>nd</i>	0.064	0.387	0.626	0.856	2.87
			[Ar] <i>nf</i>	0.000	0.014	0.029	–	
Sr <sup>+</sup>	42.89	5.813	[Ar] <i>3d<sup>10</sup>ns</i>	2.667	2.792	2.586	–	2.23
			[Ar] <i>3d<sup>10</sup>np</i>	2.112	2.264	2.021	–	
Ag	21.49	9.21	[Ar] <i>3d<sup>10</sup>nd</i>	0.650	0.998	1.017	1.500(1)	2.17
			[Ar] <i>3d<sup>10</sup>nf</i>	0.000	0.011	0.011	–	
K	31.63	5.480	[Ar] <i>3d<sup>10</sup>ns</i>	2.231	2.309	2.256(1)	1.993(55)	2.61
			[Ar] <i>3d<sup>10</sup>np</i>	1.801	1.893	1.861(2)	1.438(29)	
Na	47.29	1.001	[Ar] <i>3d<sup>10</sup>nd</i>	0.836	0.993	0.956(2)	1.341(13)	1.93
			[Ar] <i>3d<sup>10</sup>nf</i>	0.001	0.019	–	–	
Be <sup>+</sup>	153.9	0.05226	[Kr] <i>ns</i>	2.991	3.149	3.131	1.628(6)	0.85
			[Kr] <i>np</i>	2.424	2.611	2.639(1)	1.444(5)	
Ca <sup>+</sup>	50.91	3.26	[Kr] <i>nd</i>	0.972	1.347	1.347	1.673(2)	1.89
			[Kr] <i>nf</i>	0.000	0.012	0.016	–	
Mg <sup>+</sup>	80.14	0.4533	[Kr] <i>ns</i>	2.596	2.713	2.707(1)	1.332(11)	2.23
			[Kr] <i>np</i>	2.165	2.300	2.308(3)	1.260(13)	
Zn <sup>+</sup>	39.72	3.032	[Kr] <i>nd</i>	1.227	1.434	1.456(2)	1.231(7)	1.40
			[Kr] <i>nf</i>	0.001	0.033	0.069	–	
Cu	20.29	6.57	[Kr] <i>4d<sup>10</sup>ns</i>	3.436	3.570	3.534	1.918(5)	2.17
			[Kr] <i>4d<sup>10</sup>np</i>	2.881	3.040	3.024(1)	1.739(10)	
Ag	21.49	9.21	[Kr] <i>4d<sup>10</sup>nd</i>	1.486	1.841	2.001	1.282(1)	2.17
			[Kr] <i>4d<sup>10</sup>nf</i>	0.000	0.012	0.017	–	

of the paper [45], it is enough to restrict ourselves to three parameters in the Ritz formula. The value of  $\mu_l^{(ref)} \equiv \mu_{\infty l}^{(ref)}$  from Tables 1 and 2 coincides with the parameter  $\mu_l^{(0)}$ . Its accuracy is determined by the accuracy of specifying the Rydberg energy levels and the value of  $E_c$ . Three decimals are shown in the fractional parts of QDs. If the precision of  $\mu_l^{(ref)}$  is lower than above-specified, then the error is indicated in parentheses in the tables.

The quantum defects reflect the influence of the ionic core on the RE. The more the RE penetrates the core, the higher the QD. With the fixed charge of the residual ion  $z$ ,

the core size increases as the number of the electrons  $N_c$  grows. Consequently, the QD also grows for the fixed value of  $l$ . Such penetrating Rydberg states have a low orbital momentum. The  $s$ -states are always penetrating, except for the H atom and the H-like ions. As the orbital quantum number  $l$  grows, the centrifugal repulsion displaces the RE outside the core. As a result, the QD decreases, and the Rydberg state becomes non-penetrating.

The tables show the quantum defects calculated both for the potential including only the screened component  $V_{Ryd}(r) = -\phi_{scr}(r)$  and for the potential (2) additionally including the polarization component  $-\phi_{polar}(r)$  specified

**Table 2.** The same as in Table 1, but for the Cs atom and the Ba<sup>+</sup> and Hg<sup>+</sup> ions (see explanations in the text)

Atom (ion)	$E_c$ , eV	$\alpha_1$ , Bohr <sup>3</sup>	Configuration	Quantum defect $\mu_l$				$r_c$ , Bohr	$R_i$ , Bohr
				Only $\phi_{\text{scr}}$	$\phi_{\text{scr}} + \phi_{\text{polar}}$		$\mu_l^{(\text{ref})}$		
					$L_m = 1$	$L_m = 2$			
Cs	23.16	16.09	[Xe] <i>ns</i>	3.734	3.919	3.995	4.049	1.341(2)	3.16
			[Xe] <i>np</i>	3.183	3.400	3.491	3.559	1.319(1)	
			[Xe] <i>nd</i>	1.825	2.271	2.410	2.466	1.397(1)	
			[Xe] <i>nf</i>	0.055	0.204	0.298	0.034	–	
			[Xe] <i>ng</i>	0.000	0.006	0.004	0.007	–	
Ba <sup>+</sup>	35.00	10.61	[Xe] <i>ns</i>	3.315	3.457	3.536	3.576	1.118(1)	2.55
			[Xe] <i>np</i>	2.891	3.049	3.141	3.166	1.149(1)	
			[Xe] <i>nd</i>	2.008	2.223	2.341	2.369	1.156(1)	
			[Xe] <i>nf</i>	0.144	0.353	0.517	0.851(1)	1.002(1)	
			[Xe] <i>ng</i>	0.000	0.015	0.024	0.021	–	
Hg <sup>+</sup>	34.20	6.827	[Xe]4 <i>f</i> <sup>14</sup> 5 <i>d</i> <sup>10</sup> <i>ns</i>	3.997	4.101	4.182	4.153(1)	1.174(6)	3.94
			[Xe]4 <i>f</i> <sup>14</sup> 5 <i>d</i> <sup>10</sup> <i>np</i>	3.575	3.697	3.786	3.688(5)	1.452(36)	
			[Xe]4 <i>f</i> <sup>14</sup> 5 <i>d</i> <sup>10</sup> <i>nd</i>	2.699	2.861	2.972	2.836(1)	1.539(8)	
			[Xe]4 <i>f</i> <sup>14</sup> 5 <i>d</i> <sup>10</sup> <i>nf</i>	0.899	1.058	1.200	–	1.135(1)	
			[Xe]4 <i>f</i> <sup>14</sup> 5 <i>d</i> <sup>10</sup> <i>ng</i>	0.000	0.011	0.032	0.014	–	

in (25). The latter is generally a sum of the contributions of the various multipoles ( $L = 1, 2, \dots, L_m$ ). In Table 1, the core polarization 1 is restricted to the dipole component ( $L_m = 1$ ). Table 2 has a quadrupole component added ( $L_m = 2$ ).

If the pure screened potential of the nucleus provides the value of the quantum defect underestimated by several percent with respect to the NIST data, then accounting the polarization potential reduces this difference to  $\sim 0.1\%$ .

It is convenient to divide the results of the quantum defects into two sets. (i) *Atoms of the group 1 and the single-charge ions of the atoms of the group 2.*

These are alkali atoms and ions of the alkaline earth atoms, whose core has a configuration of an inert element. The calculated QDs well agree with the reference values for moderately light atoms. Specifically, starting from the *s*-states of sodium, the difference is 1% and it decreases as the atomic number grows. For example, in the Sr<sup>+</sup> ion, the difference from the reference value does not exceed 0.1%. With increase in the orbital quantum number  $l$ , this difference increases and, vice versa, the QD decreases. This feature is explained by lower penetration of RE inwards the core. The electron density in the core peripheral domain is not high enough for applicability of the TFP method.

Poor agreement with the reference data for the Li atom and the Be<sup>+</sup> ion from the beginning of the Periodic table can be explained by a small number of the electrons in the core (two). Naturally, in this situation the statistical laws practically do not appear, and the TFP method is inapplicable again. It can be additionally mentioned that in this case the QDs of the Rydberg *s*-states is less than unity, thereby indicating insufficient RE penetration in the core. One

should use traditional many-part methods here, including more precise model potentials, *ab initio* calculations, etc.

If prior to Rb and Sr<sup>+</sup>, the accuracy of the TFP method increases with the growth of the number of the core electrons, then, in case of Cs and Ba<sup>+</sup>, it decreases again (see Table 2). This paradox is caused by a xenon-like structure of the core. It consists of the closed shells and contains 56 electrons, thereby being quite sensitive to the impact of the external electric field. In this case, the expansion (8) should also additionally account for the quadrupole component as well, i.e. it should be assumed that  $L_m = 2$ . Then, the accuracy of the TFP method in the QD calculation is restored to the accuracy achievable in the atoms of the previous period for  $L_m = 1$ . The similar situation was also in the problem of tunneling ionization of xenon. Namely, accounting for the Stark shift of the energy level, that is squared in the electric field strength, is not enough. At the same time, the ionization rate is overestimated and restored to the reference values by accounting for hyperpolarizability in the Stark shift [46].

(ii) *Atoms of the group 11 and the single-charge ions of the atoms of the group 12.*

The cores of the Cu, Ag atoms and the Zn<sup>+</sup> ion have a configuration of inert gas with an extra 3*d*<sup>10</sup>-shell (see Table 1), the core of the Hg<sup>+</sup> ion has a xenon configuration with two extra 4*f*<sup>14</sup>- and 5*d*<sup>10</sup>-shells (see Table 2). The accuracy of QD calculation is comparable here with the alkali atoms and the alkaline earth ions of the same periods. However, for the copper atom, the agreement is somewhat worse.

Thus, the TFP model well reproduces the QDs of the penetrating Rydberg states in the moderately light atoms with one electron above the closed core. For the superlight atoms (ions) and weakly penetrating Rydberg states, whose QDs are below unity, the agreement with the reference data becomes worse. The quantum defects are equally determined both by the screened nucleus potential and the core polarization.

The proposed method can be formally used for QD calculation in the higher-multiplicity ions of other groups (the double ones of the groups 3, 13, the triple ones of the groups 4, 14, etc.). However, with increase in the charge of the residual ion  $z$ , the fine splitting becomes noticeably contributing. However, it is not taken into account within the framework of the TFP model due to the purely Coulomb nature of the potential  $V_{\text{Ryd}}(r)$  that is used here. Therefore, the present paper does not deal with the multiply-charged ions in order to exclude the influence of relativistic effects.

## 2.2. Polarization interaction

In this subsection, the polarization potential (25) that is numerically found by the TFP method, is replaced with the approximate analytical form (10). Both the potentials are structured so as they vanish at the origin of coordinates. The free parameter (the «cutoff» radius)  $r_c$  is selected from the condition of coincidence of the calculated QDs with its reference values. The recommended values of polarizabilities of the single-charged ions of the alkali atoms  $\alpha_1$  are taken from the article [47]. The benchmark values of  $\alpha_1$  for the doubly-charged ions of the alkaline earth atoms are given, for example, in the paper [48]. It contains both the experimental (if available) and the calculated values of the polarizabilities. Since the theoretical models usually provide underestimated values of polarizability, then maximum values have been selected from the calculated ones. Specifically, for the  $\text{Cu}^+$  and  $\text{Ag}^+$  ions, the polarizabilities were taken from [49], for  $\text{Be}^{2+}$  from [50,51], for  $\text{Mg}^{2+}$  and  $\text{Ca}^{2+}$  from [52], for  $\text{Sr}^{2+}$  and  $\text{Ba}^{2+}$  from [53]. The polarizabilities of the  $\text{Zn}^{2+}$  and  $\text{Hg}^{2+}$  ions were calculated by the TFP method according to (24). The polarizabilities found with the TFP method for the neutral atoms and the single- and doubly-charged ions with the number of electrons from 2 to 92 were analyzed in the paper [28]. They turned out to be somewhat underestimated as compared to the reference values as in the case of other calculation methods. The results of fitting of  $r_c$  are also given in Tables 1 and 2.

An important criterion of internal consistency of the potential approach is independence of the potential parameters on the energy and the orbital quantum number (in the central field). It follows from the general principles of the quantum mechanics. The studied case is limited by the low energies of the REs, so it is impossible to estimate the dependence of  $r_c$  on the energy. However, the tabulated results make it possible to estimate the dependence of

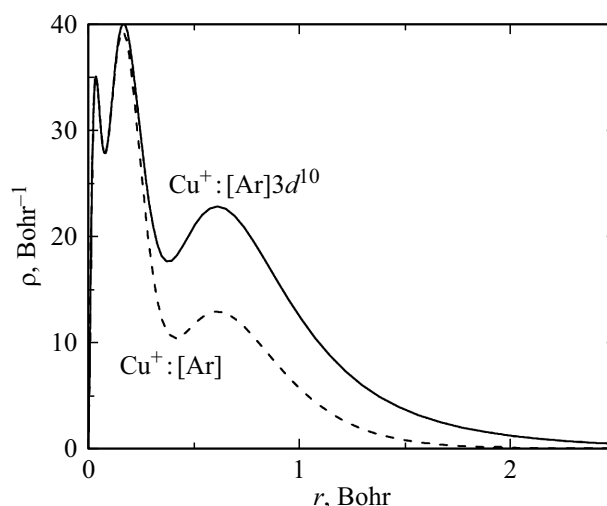


**Figure 2.** Radial distribution of the electron density in the core of the atom Cu. The dashed line means the contribution of the argon-like configuration. The calculation was performed with the Hartree–Fock method.

$r_c$  on  $l$ . The «cutoff» radii coincide with each other within 15% only for the penetrating Rydberg states in the many-electron atoms of the alkali metals and the ions of the alkaline earth metals. Despite good compliance of the QDs with the reference data, the parameter  $r_c$  turns out to be strongly dependent on  $l$  in the Na atom and the  $^+$  ion, which is possibly stipulated by a relatively small number of the electrons in the core (ten electrons). In the weakly penetrating states of REs,  $r_c$  becomes substantially dependent on  $l$  as well or the quantity is absent. Here, the core electrons' density is so low that individual properties of the atoms prevail over the statistical ones.

In the atoms and the ions of the groups 11 and 12, whose core has an external  $d^{10}$  shell ( $\text{Cu}$ ,  $\text{Zn}^+$ ,  $\text{Ag}$ ,  $\text{Hg}^+$ ), the calculation of  $r_c$  with the TFP method is either impossible or again results in the strong dependence of  $r_c$  on  $l$  in the penetrating Rydberg states (for  $\text{Zn}^+$ ,  $\text{Ag}$  and  $\text{Hg}^+$ , the difference between the neighbor values of  $r_c$  exceeds 25%). The possible cause of such behavior of  $r_c$  is that the core has the external  $d^{10}$ -shell, which is absent in the atomic configurations of the noble gases and broadens a peripheral domain of the core with the low electron density, which is important for calculations of the QDs and the polarization characteristics, where the TFP model is actually inapplicable (Fig. 2 for the Cu core). In other words, the TFP model is valid if the electron density is quite high and the peripheral domain is quite narrow.

In most cases, the parametrization of polarization interaction by the formula (11) cannot provide the values of  $r_c$ , since this potential is substantially «shallow» as compared to (10). The polarization potential from the paper [31] has been taken in an incompletely correct form (12) (all the polarizabilities were calculated in [31]

with the TFP method). Unlike (10) and (11), it has a non-zero value in the origin of coordinates and provides  $r_c$ , which are by  $\sim 20\%$  smaller as compared to (10). However, the potential (12) keeps all the trends in the change of  $r_c$  from state to state, as given by the potential (10).

Thus, the fitting of the polarization potential parameter  $r_c$  is a more sensitive tool for testing the TFP method as compared to the QD calculation. It reduces the applicability of the TFP method to the Rydberg states of quite heavy atoms and ions only, whose core has a configuration of an atom of the inert gas, starting from argon.

It is interesting to compare the «cutoff» radius  $r_c$  with the ionic radius  $R_i$ , which defines a length of the ionic chemical bond in the molecules [54] (the present paper takes all the ionic radii  $R_i$  from the database [55] for the coordination number VI, since it is valid almost for all the ions specified in the base). Under the conditions of applicability of the TFP method, the ratio  $r_c/R_i$  will stay in a quite narrow range from 0.4 to 0.6. In other words,  $r_c$  lies inside the core and has an order of its radius. A small growth of  $r_c/R_i$  with increase in  $N_c$  can be explained by the total increase in the core electron density. However, the parameter  $r_c$  lies outside the specified range in the Cs atom and the  $\text{Ba}^+$  ion. The possible cause of this paradox is discussed in the previous subsection. It is caused by the high sensitivity of the xenon-like core to external influences. In this case the analytical expression (10) should have been replaced by

$$\phi_{\text{polar}}(r) \approx \frac{\alpha_1}{2r^4} \left(1 - e^{-r^6/r_c^6}\right) + \frac{\alpha_2 + \beta'}{2r^6} \left(1 - e^{-r^{10}/r_c^{10}}\right),$$

where  $\alpha_2$  is the hyperpolarizability of the core (in the terms of [28]),  $\beta'$  is a non-adiabatic free parameter. However, an additional problem of consistent selection of  $r_c$  and  $\beta'$  arises here.

The Fr atom and the  $\text{Ra}^+$  ion are not considered here due to instability of their nuclei.

The proposed method of testing the TFP method can be transferred to the other density functionals as well. Presently, 128 standard density functionals are known [56]. Some of them correctly reproduce the low electron density in the peripheral domains. For example, the mPW1PBE functional is suitable for calculating the dynamic polarizabilities of the diatomic molecules [57]. It would be interesting to study such functionals using the proposed methods.

## Conclusion

Within the framework of the model-potential approach, the WKB formula of the quantum defect for the Rydberg electron is derived. Using the model potential obtained within the Thomas–Fermi–Patil method, the quantum defects of the atoms with one electron above the closed core shells have been calculated. It has demonstrated that the screened and the polarization component of the RE potential should be jointly taken into

account. In case of the heavy atoms, the highest multipole components of polarization potential of the core can noticeably affect the RE motion. The values of the cutoff radius have been found in the formula of polarization potential for some alkali atoms and similar ions.

The calculation results have been compared to the reference data, thereby establishing the boundaries of applicability of the TFP method for the RE: the atom or ion must have a core with the configuration of the inert element, the Rydberg state must significantly penetrate the core, i.e. the QD value must exceed unity (usually, these are the  $s$ -,  $p$ - and  $d$ -states). These requirements are fulfilled for the stable alkali atoms K, Rb, Ca of the group 1 and the alkaline earth ions  $\text{Ca}^+$ ,  $\text{Sr}^+$ ,  $\text{Ba}^+$  of the group 2. The «cutoff» radius demonstrated the high sensitivity to selecting the RE model potential as compared to the QD. If the closed core contains the outermost  $d^{10}$ - and/or  $f^{14}$ -shells (the subgroup 11 and 12 of the Periodic table), then the «cutoff» radius either substantially depends on the RE orbital momentum or is absent. Under the conditions of applicability of the TFP method, the «cutoff» radius is 0.4 – 0.6 of the respective ionic radius.

The proposed approach can be applied in testing the accuracy of the various density functionals and the model potentials. The obtained results can be used as an initial approximation in precise calculations of the characteristics of the Rydberg atoms and ions, and when there are not more accurate values in the literature and the databases.

## Funding

This study is financially supported by the Ministry of Science and Higher Education of the Russian Federation (the project FZGU-2023-0007).

## Conflict of interest

The author declares that he has no conflict of interest.

## Appendix

After the substitution (33), the integral (34) is transformed into the form:

$$\begin{aligned} \int_R^{r_2} P_{nl}^{(0)}(r) dr &= v_{nl} \epsilon_{nl}^2 \int_{\varphi_{nl}}^{\pi} \frac{\sin^2 \varphi}{1 - \epsilon_{nl} \cos \varphi} d\varphi = v_{nl} \left\{ \varphi + \epsilon_{nl} \cos \varphi \right. \\ &\quad \left. - 2\sqrt{1 - \epsilon_{nl}^2} \arctan \left[ \frac{\sqrt{1 - \epsilon_{nl}^2}}{1 - \epsilon_{nl}} \tan \frac{\varphi}{2} \right] \right\} \Bigg|_{\varphi=\varphi_{nl}}^{\varphi=\pi} \\ &= \pi(v_{nl} - \mathcal{L}_l) - v_{nl}(\varphi_{nl} + \epsilon_{nl} \sin \varphi_{nl}) \\ &\quad + 2\mathcal{L}_l \arctan \left[ \frac{\mathcal{L}_l}{v_{nl}(1 - \epsilon_{nl})} \tan \frac{\varphi_{nl}}{2} \right]. \end{aligned}$$

If the parameters  $\mathcal{L}_l/v_{nl}$  and  $zR/v_{nl}^2$  are small, then the elements of this expression can be expanded into the Taylor series:

$$\begin{aligned}\epsilon_{nl} &\approx 1 - \frac{\mathcal{L}_l^2}{2v_{nl}^2}, & \cos \varphi_{nl} &\approx 1 + \frac{\mathcal{L}_l^2 - 2zR}{2v_{nl}^2}, \\ \sin \varphi_{nl} &= \sqrt{1 - \cos^2 \varphi_{nl}} \approx \frac{\mathcal{L}_l \Xi_l}{v_{nl}} \ll 1, \\ \varphi_{nl} &\approx \sin \varphi_{nl} \approx \frac{\mathcal{L}_l \Xi_l}{v_{nl}}, & \tan \frac{\varphi_{nl}}{2} &\approx \frac{\varphi_{nl}}{2} \approx \frac{\mathcal{L}_l \Xi_l}{2v_{nl}}, \\ \arctan \left[ \frac{\mathcal{L}_l}{v_{nl}(1 - \epsilon_{nl})} \tan \frac{\varphi_{nl}}{2} \right] &\approx \arctan \Xi_l.\end{aligned}$$

Here,  $\Xi_l$  is defined in (36).

Finally, we obtain the expression (35).

## References

- [1] T.F. Gallagher. *Rydberg atoms. Cambridge Monographs on Atomic, Molecular and Chemical Physics*. (Cambridge University Press, Cambridge, 1994). URL: <https://www.cambridge.org/core/books/rydberg-atoms/B610BDE54694936F496F59F326C1A81B>
- [2] N. Šibalić, C.S. Adams. *Rydberg physics*, ser. 2399-2891. (IOP Publishing, Bristol, 2018). DOI: 10.1088/978-0-7503-1635-4
- [3] N.D. Guise, J.N. Tan, S.M. Brewer, C.F. Fischer, P. Jönsson. *Phys. Rev. A*, **89** (4), 040502 (2014). DOI: 10.1103/PhysRevA.89.040502
- [4] Y.N. Gnedin, A.A. Mihajlov, Lj.M. Ignjatović, N.M. Sakan, V.A. Srećković, M.Yu. Zakharov, N.N. Bezuglov, A.N. Klycharev. *New Astron. Rev.*, **53** (7), 259 (2009). DOI: 10.1016/j.newar.2009.07.003
- [5] J. Neukammer, H. Rinneberg, U. Majewski. *Phys. Rev. A*, **30** (2), 1142 (1984). DOI: 10.1103/PhysRevA.30.1142
- [6] G. Vitrant, J.M. Raimond, M. Gross, S. Haroche. *J. Phys. B: At. Mol. Phys.*, **15** (2), L49 (1982). DOI: 10.1088/0022-3700/15/2/004
- [7] R. Heidemann, U. Raitzsch, V. Bendkowsky, B. Butscher, R. Löw, L. Santos, T. Pfau. *Phys. Rev. Lett.*, **99** (16), 163601 (2007). DOI: 10.1103/PhysRevLett.99.163601
- [8] N. Duarte Gomes, B. da Fonseca Magnani, J.D. Massayuki Kondo, L.G. Marcassa. *Atoms*, **10** (2), 58 (2022). DOI: 10.3390/atoms10020058
- [9] J.D. Pritchard, D. Maxwell, A. Gauguier, K.J. Weatherill, M.P.A. Jones, C.S. Adams. *Phys. Rev. Lett.*, **105** (19), 193603 (2010). DOI: 10.1103/PhysRevLett.105.193603
- [10] O. Firstenberg, T. Peyronel, Q.-Y. Liang, A.V. Gorshkov, M.D. Lukin, V. Vuletić. *Nature*, **502** (10), 71 (2013). DOI: 10.1038/nature12512
- [11] E.A. Yakshina, D.B. Tretyakov, I.I. Beterov, V.M. Entin, C. Andreeva, A. Cinins, A. Markovski, Z. Iftikhar, A. Ekers, I.I. Ryabtsev. *Phys. Rev. A*, **94** (4), 043417 (2016). DOI: 10.1103/PhysRevA.94.043417
- [12] A. Mazalam, K. Michulis, I.I. Beterov, N.N. Bezuglov, A.N. Klycharev, A. Ekers. *Opt. Spectr.*, **127** (3), 375 (2019). DOI: 10.1134/S0030400X19090200
- [13] S. Saakyan, N. Morozov, V. Sautenkov, B.B. Zelener. *Atoms*, **11** (4), 73 (2023). DOI: 10.3390/atoms11040073
- [14] A.V. Taichenachev, V.I. Yudin, S.N. Bagayev. *Phys. – Uspekhi*, **59** (2), 184 (2016). DOI: 10.3367/UFNe.0186.201602j.0193
- [15] E.F. Stelmashenko, O.A. Klezovich, V.N. Baryshev, V.A. Tishchenko, I.Yu. Blinov, V.G. Palchikov, V.D. Ovsyanikov. *Opt. Spectrosc.*, **128** (8), 1067 (2020). DOI: 10.1134/S0030400X20080366
- [16] W. Clark, C.H. Greene. *Phys. Rev. A*, **56** (1), 403 (1997). DOI: 10.1103/PhysRevA.56.403
- [17] A.I. Al-Sharif, R. Resta, C.J. Umrigar. *Phys. Rev. A*, **57** (4), 2466 (1998). DOI: 10.1103/PhysRevA.57.2466
- [18] C.B. Xu, X.P. Xie, R.C. Zhao, W. Sun, P. Xue, Z.P. Zhong, W. Huang, X.Y. Xu. *J. Phys. B: At. Mol. Opt. Phys.*, **31** (24), 5355 (1998). DOI: 10.1088/0953-4075/31/24/016
- [19] N. Zheng, D. Ma, R. Yang, T. Zhou, T. Wang, S. Han. *J. Chem. Phys.*, **113** (5), 1681 (2000). DOI: 10.1063/1.481969
- [20] J. Migdalek. *At. Data Nucl. Data Tables*, **135–136**, 101355 (2020). DOI: 10.1016/j.adt.2020.101355
- [21] V.V. Kuzenov, S.V. Ryzhkov, V.V. Shumaev. *Prob. Atomic Sci. Technol.*, **95**, 97 (2015).
- [22] V.V. Kuzenov, S.V. Ryzhkov, V.V. Shumaev. *Prob. Atomic Sci. Technol.*, **98**, 53 (2015).
- [23] P. Gombás. *Die statistische theorie des atoms und ihre anwendungen*. (Springer-Verlag, Luxemburg, 1949), sect. 24.
- [24] D.A. Kirzhnits, Y.E. Lozovik, G.V. Shpatakovskaya. *Sov. Phys. – Uspekhi*, **18** (9), 649 (1975). DOI: 10.1070/PU1975v018n09ABEH005199
- [25] G.V. Shpatakovskaya. *Phys. – Uspekhi*, **55** (5), 429 (2012). DOI: 10.3367/UFNe.0182.201205a.0457
- [26] S. Seriy. *OJMSi*, **3** (3), 96 (2015). DOI: 10.4236/ojmsi.2015.33010
- [27] S.H. Patil. *J. Phys. B: At. Mol. Opt. Phys.*, **22** (13), 2051 (1989). DOI: 10.1088/0953-4075/22/13/009
- [28] S.H. Patil. *At. Data Nucl. Data Tables*, **71** (1), 41 (1999). DOI: 10.1006/adnd.1998.0799
- [29] L. Neale, M. Wilson. *Phys. Rev. A*, **51** (5), 4272 (1995). DOI: 10.1103/PhysRevA.51.4272
- [30] Z. Xianzhou, S. Jinfeng, L. Yufang. *J. Phys. B: At. Mol. Opt. Phys.*, **25** (8), 1893 (1992). DOI: 10.1088/0953-4075/25/8/021
- [31] A.S. Kornev, B.A. Zon. *J. Phys. B: At. Mol. Opt. Phys.*, **36** (19), 4027 (2003). DOI: 10.1088/0953-4075/36/19/011
- [32] A. Kramida, Yu. Ralchenko, J. Reader, and NIST ASD Team. *NIST Atomic Spectra Database (ver. 5.10)* [Electronic resource]. URL: <https://physics.nist.gov/asd>
- [33] I.S. Madjarov, J.P. Covey, A.L. Shaw, J. Choi, A. Kale, A. Cooper, H. Pichler, V. Schkolnik, J.R. Williams, M. Endres. *Nat. Phys.*, **16**, 857 (2020). DOI: 10.1038/s41567-020-0903-z
- [34] P.G. Burke. *Potential scattering in atomic physics* (Springer US, New York, 2012), ch. 6, eq. 176.
- [35] L.H. Thomas. *Proc. Camb. Phil. Soc.*, **23**, 542 (1926). DOI: 10.1017/S0305004100011683
- [36] E. Fermi. *Z. Phys.*, **48**, 73 (1928).
- [37] P.A.M. Dirac. *Proc. Camb. Phil. Soc.*, **26**, 376 (1930). DOI: 10.1017/S0305004100016108
- [38] J. Schwinger. *Phys. Rev. A*, **24** (5), 2353 (1981). DOI: 10.1103/PhysRevA.24.2353
- [39] H.J. Brudner, S. Borowitz. *Phys. Rev.*, **120** (6), 2053 (1960). DOI: 10.1103/PhysRev.120.2053
- [40] E. Fermi, E. Amaldi. *Mem. Accad. d'Italia*, **6**, 119 (1934).
- [41] I.I. Beterov, I.I. Ryabtsev, D.B. Tretyakov, V.M. Entin. *Phys. Rev. A*, **79** (5), 052504 (2009). DOI: 10.1103/PhysRevA.79.052504
- [42] L.D. Landau, E.M. Lifshitz. *Quantum mechanics, nonrelativistic theory* (Pergamon, Oxford, 1991), sect. 49

- [43] L.D. Landau, E.M. Lifshitz. *Mechanics* (Elsevier Science, Amsterdam, 1982), sect. 15.
- [44] V.V. Kazakov, V.G. Kazakov, O.I. Meshkov, A.S. Yatsenko. *Phys. Scr.*, **92**, 105002 (2017). DOI: 10.1088/1402-4896/aa822e
- [45] E. Biémont, P. Quinet, V. Van Renterghem. *J. Phys. B: At. Mol. Opt. Phys.*, **31** (24), 5301 (1998). DOI: 10.1088/0953-4075/31/24/012
- [46] A.S. Kornev, I.M. Semiletov, B.A. Zon. *J. Phys. B: At. Mol. Opt. Phys.*, **47** (20), 204026 (2014). DOI: 10.1088/0953-4075/47/20/204026
- [47] A.S. McNeill, K.A. Peterson, D.A. Dixon. *J. Chem. Phys.*, **153** (17), 174304 (2020). DOI: 10.1063/5.0026876
- [48] J. Mitroy, M.S. Safronova, C.W. Clark. *J. Phys. B: At. Mol. Opt. Phys.*, **43** (20), 202001 (2010). DOI: 10.1088/0953-4075/43/20/202001
- [49] P. Neogrády, V. Kellö, M. Urban, A. Sadlej. *Theor. Chim. Acta*, **93**, 101 (1996). DOI: 10.1007/BF01113551
- [50] W.R. Johnson, K.T. Cheng. *Phys. Rev. A*, **53** (3), 1375 (1996). DOI: 10.1103/PhysRevA.53.1375
- [51] A.K. Bhatia, R.J. Drachman. *Can. J. Phys.*, **75** (1), 11 (1997). DOI: 10.1139/p96-132
- [52] U. Öpik. *Proc. Phys. Soc.*, **92** (3), 566 (1967). DOI: 10.1088/0370-1328/92/3/308
- [53] W. Johnson, D. Kolb, K.-N. Huang. *At. Data Nucl. Data Tables*, **28** (2), 333 (1983). DOI: 10.1016/0092-640X(83)90020-7
- [54] R.D. Shannon. *Acta Cryst. A*, **32** (5), 751 (1976). DOI: 10.1107/S0567739476001551
- [55] R. Grimes, N. Kuganathan, C. Galvin, M. Jackson, A. Hodgson, A. Kenich, T.Y. Ren. *Database of Ionic Radii* [Electronic source]. URL: <http://abulafia.mt.ic.ac.uk/shannon/>
- [56] M.G. Medvedev, I.S. Bushmarinov, J. Sun, J.P. Perdew, K.A. Lyssenko. *Science*, **355** (6320), 49 (2017). DOI: 10.1126/science.aah5975
- [57] A.S. Kornev, K.I. Suvorov, V.E. Chernov, I.V. Kopytin, B.A. Zon. *Opt. Spectr.*, **127** (5), 798 (2019). DOI: 10.1134/S0030400X1911016X.

*Translated by M.Shevelev*